Passivation of Metals and Semiconductors, and Properties of Thin Oxide Layers
P. Marcus and V. Maurice (Editors)

Surface Characterization of 1018 Carbon Steel in Borate Medium by *in-situ* Electrochemical Scanning Tunneling Microscopy

Ignacio González[a,*], Román Cabrera-Sierra[a,b], Nikola Batina[a]

[a]*Universidad Autónoma Metropolitana-Iztapalapa. Departamento de Química. Apartado Postal 55-534. 09340 México, D.F. (MEXICO). igm@xanum.uam.mx*
[b]*Escuela Superior de Ingeniería Química e Industrias Extractivas (ESIQIE-IPN) Academia de Química Analítica, Edificio Z5. A.P:75-874, C.P. 07338, México, D.F. (MEXICO).*

Abstract - Microstructures of low carbon steel are ferrite (Fe-α) and pearlite (alternate mixture of Fe-α and Fe_3C) and each one has its own oxidation mechanism. These two phases were identified using *in-situ* electrochemical scanning tunneling microscopy (ECSTM). Real time images were obtained during the immersion of 1018 carbon steel probes in 0.642 M H_3BO_3 and 0.1 M NaOH, pH = 7.8. Two different corrosion mechanisms were identified and correlated with the observed surface changes.

Keywords : ECSTM, Corrosion, Carbon Steel, Pearlite, Ferrite .

1. Introduction

Carbon steel corrosion in aqueous media is one of the most studied systems for its impact on the chemical industry. Usually, the carbon steel - aqueous media interface has been studied *in-situ* using different electrochemical and *ex-situ* using different spectroscopic techniques [1-8]. In particular, the surface composition of the low carbon steel is strongly related to its oxidation processes. In dependence on the fabrication process, a carbon steel surface has different phases such as ferrite, Fe_α (iron rich phase), and pearlite (sequential arrangement of ferrite and iron carbide, Fe_3C) [9]. Usually, corrosion studies of a steel interface in an aqueous medium do not consider separate oxidation mechanism for each phase, thereby obtaining only global information on the

mechanism relative to that interface [1-8]. This work focus on determination and characterization of corrosion of ferrite and pearlite on a steel sample, in the borate medium, using an *in-situ* Electrochemical Scanning Tunneling Microscopy (ECSTM). The real time monitoring of changes in the steel surface topography, allows to understand each phase oxidation as well as their influence on the global carbon steel corrosion process.

2. Results and Discussion

The experimental conditions and methodology of the ECSTM image recording process were described in details in our previous work [10]. It is important to indicate that the experimental methodology proposed in this work for surface characterization of 1018 carbon steel in borate medium using in-situ ECSTM technique is different from that reported in other works [11-13]. In the literature, such characterization is carried out after cleaning the surface of corrosion products formed during its preparation (through an imposed cathodic potential). However, here it is proposed that the surface is studied with no prior electrochemical treatment. Moreover, this work focuses on studying the corrosion process of steel in aqueous medium using the time of immersion (at early stages of corrosion) in order to differentiate the reactivity of distinct microstructures on the basis of oxidation mechanism of each steel phase. Nevertheless, it is important to indicate that such goal can be achieved only if the corrosion process images are obtained at short immersion times, since longer times make the process visualization difficult. Mechanism of the imaging of iron oxides is still not clear for us. We believe the iron oxides are conductives specially magnetite. However we also believed that specially important for imaging obtention is the thickness of the oxide films, which is not defined in our work. After a systematic analysis of the major part of the sample surface, at different immersion time in a borate medium, two different types of surface with characteristic structures were identified (pearlite and ferrite) and selected as model surfaces for further studies of the corrosion behavior. A set of images presented in Figures 1 (a-b), is related to characterization of the pearlite phase on the 1018 carbon steel surface using the ECSTM technique, in a borate medium. The key issue was an identification of the periodical arrangement (linear rows) characteristic for the pearlite phase, of the carbon steel [14,15]. The surface topography (surface features) observed in our ECSTM images is very similar to surface microstructure seen by Scanning Electron Microscopy (SEM), reported and describe in details in previous works [14,15]. In agreement with this previous work, we also found that distance between the observed pearlite rows in SEM (0.095 μm) and ECSTM images (0.1 μm) is identical. As a further step in our study, the part of the sample surface identified as a pearlite phase, was a subject of continuos monitoring during the oxidation progress as a function of the immersion time (characterization time). Figure 1b shows the progress of the oxidation of the pearlite phase after 84 min of immersion in the

borate solution. The sample surface is covered by granular features which size varies from 0.4 to 1 μm.

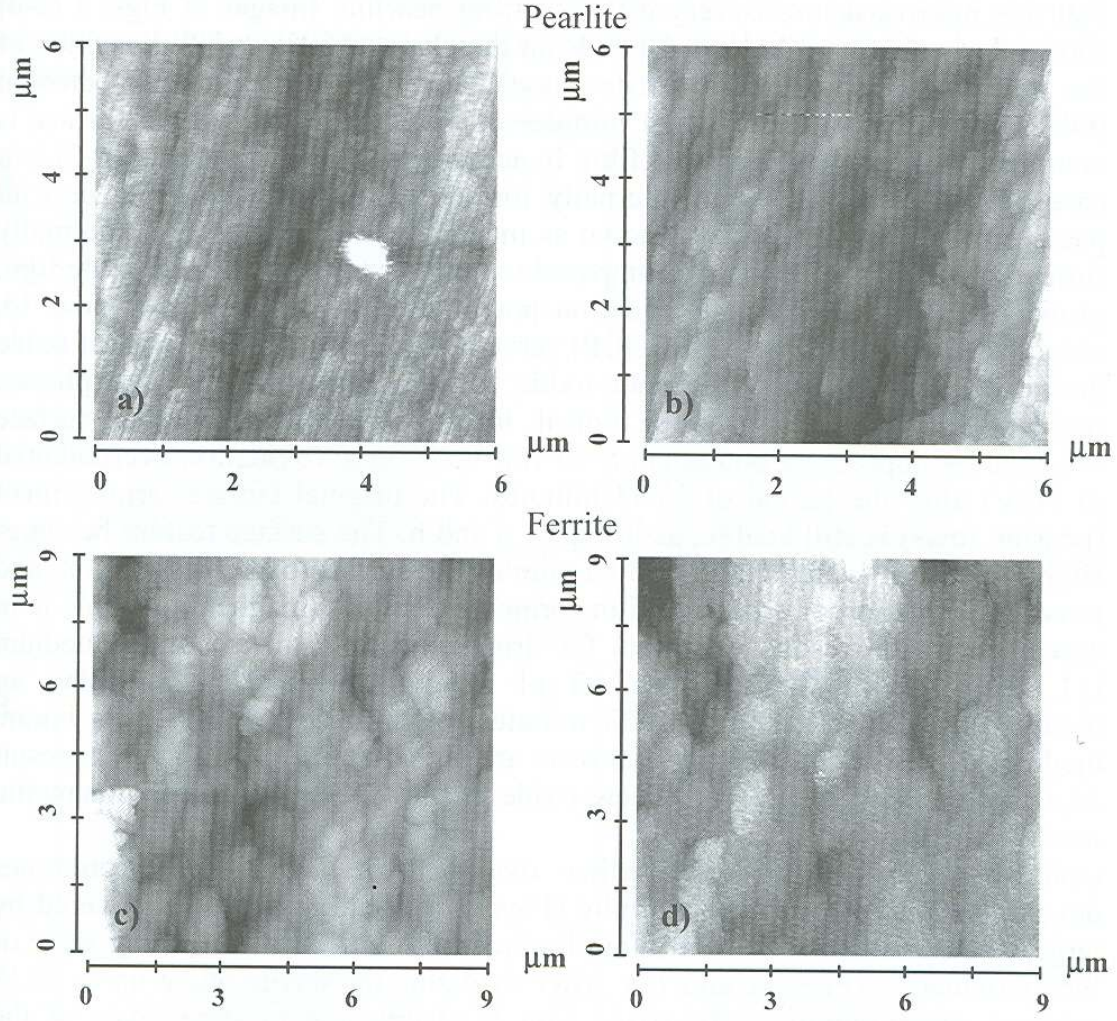

Figure 1. *In-situ* ECSTM images of 1018 carbon steel immersed in 0.642 M H_3BO_3 and 0.1 M NaOH, pH = 7.8, after different immersion time. **Pearlite phase**: **a)** t =11.5 min (Z scale: 0 – 27.5 nm), **b)** t = 84 min (Z scale: 0 – 22.5 nm). **Ferrite phase**: **c)** t = 23 min (Z scale: 0 – 20 nm), **d)** t = 36 min (Z scale: 0 – 22.5 nm). All images were recorded at the Open Circuit Potential (-0.125 V), with a bias potential of -0.180 V, a tip potential of –0.305 V and tip current of 2 - 3 nA.

The oxide growth occurs along the preferential directions determinate by the texture and the microstructure of the previous pearlite layer. It persists even at the larger time of immersion with more progress of oxidation. The width and the distance between the original pearlite rows increase as a function of the immersion time. The observed surface topography changes a typical for low oxidative properties of the pearlite phase of the steel surface. Distinguished surface topography without linear alignment, with larger granular features (1-2

μm) and with significantly higher magnitude of the surface perturbations during the oxidation process, was observed for ferrite (Fe-α) phase (Figs. 1 (c-d)). Note that this microstructure is very different from pearlite. Images at Figs. 1 (a-d) shows that oxide morphology depends on the characteristic and composition of the steel surface (pearlite vs. ferrite phase). However, at open circuit potential (OCP) conditions, after few first minutes of immersion, the sample surface is completely covered by the oxide film. In accordance to the literature [16-21], in case of both phases, it is an internally formed oxide film (barrier layer with passive properties [11,12,22]) known as magnetite. Furthermore this internally formed iron oxide film will be compared with the externally formed oxide film, grown by applying external oxidation potentials. Images at Figs 1b and 1d, recorded at –0.125 V vs. NHE (OCP) serve as the reference for external oxide growth monitoring over the inner oxide film of pearlite and ferrite phases, respectively. Figure 2a shows typical image of oxidized pearlite surface obtained by imposing a potential of – 0.120 V vs. NHE (oxidation overpotential of 5mV) after the period of 33.33 minutes. The original laminar arrangement (pearlite rows) is still visible, as in Figs.1 a and b. The surface feature becomes slightly smaller, which could be first sign of the surface oxide dissolution, and possibly formation of a passive film formed externally (maghemite). This is in agreement with results reported for iron oxidation in a borate medium [11,12,22]. Figure 2b shows a set of images obtained by imposing an overpotential of 65 mV after 3.33 minutes to the pearlite phase in a borate medium. Detail analysis shows that rows are higher and slightly wider, as result of a preferential growth of the new oxide at the top of the pearlite/magnetite lines.

Contrasting to pearlite, the further oxidation of ferrite phase promotes development of different topography (Figs. 2 c and d). Surface is covered by large oxide grains (1.5 – 2 μm) not observed before in the case of any stage of ferrite oxidation (Figs. 1c and 1d). After oxidizing the ferrite phase up to 33.33 minutes, deterioration of the oxide film is visible due to appearance of the nanometric size pits. We suppose that it is result of rather complex mechanism of formation of the external oxide film, which is associated to maghemite. However, at this point we could not speculate more about mechanisms involved in this process. Here, we just could conclude that observed changes in the surface topography differs significantly for different phases: pearlite and ferrite in case of formation of internal and external iron oxide layers. In other words ECSTM appears to be a useful tool for in-situ monitoring and characterization of the steel surface oxidation.

3. Conclusion

Using ECSTM it was successfully characterized the state of the electrode surface, identified phases at the steel sample, determinate surface morphology characteristics and by systematic monitoring of topography change, it was

possible to determinate and differentiate oxidation mechanisms of different steel phases (pearlite vs. ferrite). In particular it is interesting a visualization of development of internal and external oxide layers, which open new possibilities in studies of the oxidation processes at the micro and nanoscale level, at in-situ conditions.

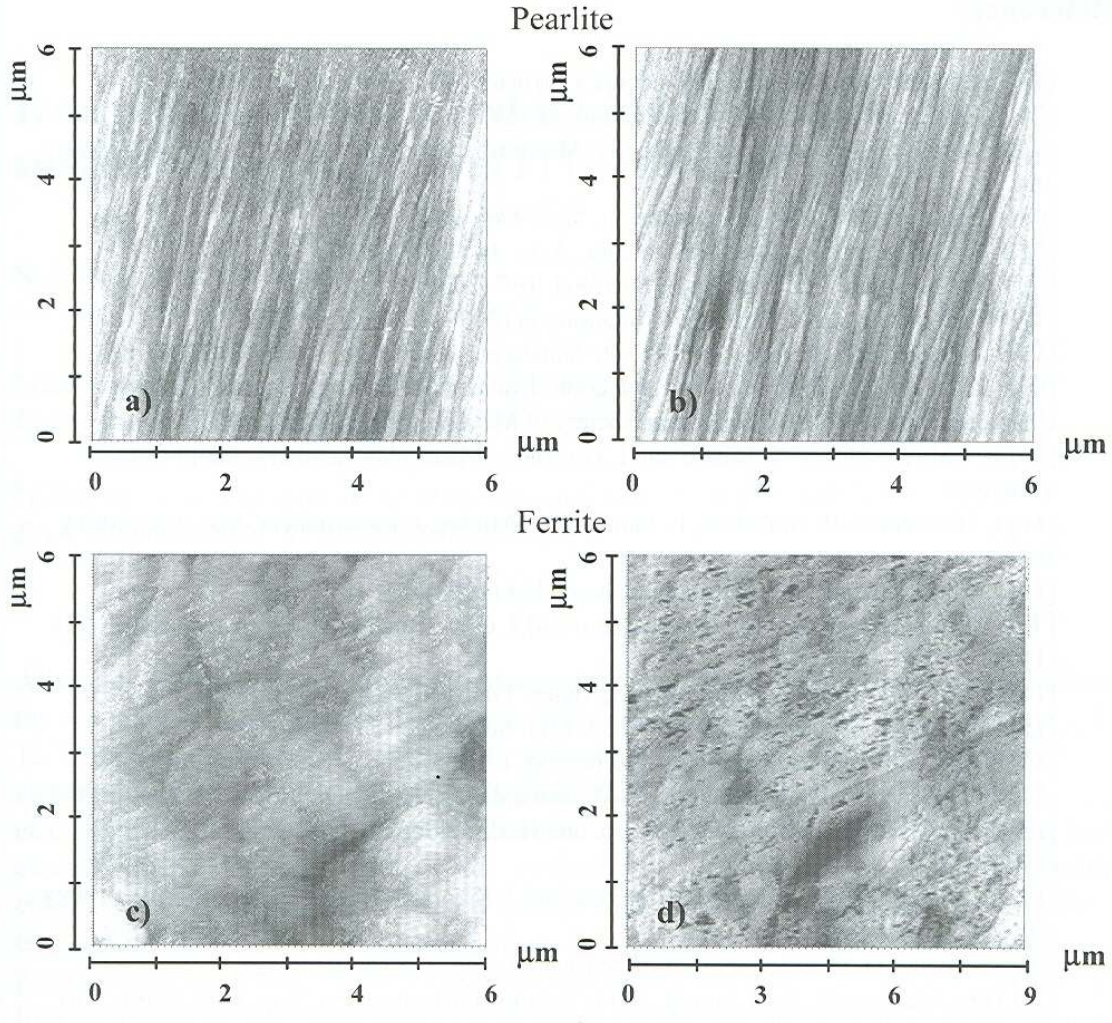

Figure 2. Typical ECSTM images (6µm x 6µm) recorded after applying different oxidation overpotentials to the different carbon steel phases in contact with the borate medium (pH=7.8). **Pearlite, a)** overpotential 5 mV after 33.33 minutes (Z scale: 0 – 25 nm, tip potential –0.300 V), **b)** overpotential 65 mV after 3.33 minutes (Z scale: 0 – 50 nm, tip potential –0.120V). **Ferrite, c)** overpotential 150 mV after 3.33 minutes (Z scale: 0 – 27 nm, tip potential –0.155 V), **d)** overpotential 170 mV after 33.33 minutes (Z scale: 0 - 45 nm, tip potential –0.135 V). The usual imaging conditions were a bias potential of -0.180 V and tip current of 2 - 3 nA.